Prepared for the National Institutes of Health
National Institute of Neurological Disorders and Stroke
Division of Stroke, Trauma and Neurodegenerative Disorders
Neural Prosthesis Program
Bethesda, MD 20892

Microstimulation of the Lumbosacral Spinal Cord: Mapping

NIH-NINDS-NO1-NS-8-2300

Quarterly Progress Report #4

Period Covered: 1 July, 1999 - 30 September, 1999

Principal Investigator: Warren M. Grill, Ph.D.

Co-Investigators: Musa A. Haxiu, M.D., Ph.D.
Michel A. Lemay, Ph.D.

Department of Biomedical Engineering
Case Western Reserve University
Cleveland, OH 44106-4912

ABSTRACT

The objectives of this research are to determine the anatomical locations of spinal neurons involved in control of the genitourinary and hindlimb motor systems, and to determine the physiological responses evoked in the genitourinary and hindlimb motor systems by intraspinal microstimulation. During this quarter we made progress toward both of these objectives. We continued a series of experiments to characterize the hindlimb motor responses evoked by microstimulation of the lumbar spinal cord. Specifically, we measured the endpoint forces evoked by intraspinal microstimulation of the contralateral lumbar spinal cord in decerebrate cats, and compared these response to those obtained by ipsilateral microstimulation. We also continued development of an electrical technique to localize neurons in the spinal cord using recordings of electrical potential on the surface of the spinal cord. During this quarter we examined the solutions for the potentials generated in a two concentric cylindrical volume conductor models of the spinal cord, and developed the solution for a new model that accounts for the anistropy of the outer cylinder, representative of the white matter.

INTRODUCTION

Electrical stimulation of the nervous system is a means to restore function to individuals with neurological disorders. The objective of this project is to investigate the feasibility of neural prosthetics based on microstimulation of the spinal cord with penetrating electrodes. Specifically, chemical and viral retrograde tracers, immediate early gene expression, and immunocytochemistry are used to determine the locations and neurochemical identity of neurons in the spinal cord that control genitourinary and motor functions in the male cat. Microstimulation with penetrating activated iridium microelectrodes is used to determine the physiological effects in the genitourinary and motor systems of activation of different neural populations. The results of this project will provide data important to understanding neural control of genitourinary and motor functions, answer fundamental questions about microstimulation of the spinal cord, and lead to development of a new generation of neural prosthetics for individuals with neurological impairments.

PROGRESS IN THIS QUARTER

During the second quarter of this contract we continued a series of experiments to measure the endpoint force produced at the hindlimb by microstimulation of the lumbar

spinal cord. We also continued work on an electrical technique to localize neuronal populations within the spinal cord. Below each of our accomplishments is summarized.

Hindlimb Motor Responses Evoked by Intraspinal Microstimulation

We are conducting a series of experiments to characterize the hindlimb motor responses evoked by microstimulation. In these experiments rather than recording single joint responses, we are recording the net force at the endpoint of the hindlimb. During the period covered by this report, we studied the motor responses evoked by intraspinal microstimulation of the contralateral lumber enlargement of the spinal cord, in contrast to our previous experiments, which were conducted with ipsilateral microstimulation.

METHODS

The endpoint forces evoked at the paw by microstimulation of the lumbar spinal cord were recorded in unanesthetized decerebrate cats. All animal care and experimental procedures were according to NIH guidelines and were approved by the Institutional Animal Care and Use Committee of Case Western Reserve University.

Experimental Preparation

Animals were anesthetized with ketamine HCl (Ketaset, 15-30 mg/kg, IM), intubated, and anesthesia was maintained with gaseous halothane (1-2 %) in oxygen. A laminectomy was made to expose the lumbosacral spinal cord, and the contralateral (left) hindlimb was denervated by transecting the femoral, obturator, and sciatic nerves. Denervation was done to prevent mechanical coupling of responses in the left limb to the force sensor to which the right limb was attached. The animal was mounted in a frame with pins at the hips, the head in a headholder, and vertebral clamps at L3 and S1. The femur was fixed with a steel pin, and the paw was attached to a gimbal mounted on a 3-axis force/moment transducer (Nano-17, ATI Inc., Garner, NC). The force transducer was mounted on a cartesian manipulator that allowed positioning of the force sensor throughout the workspace of the lower leg and paw, while the gimball permits the rotation of the ankle when the limb is moved. Fine bifilar wire electrodes were inserted into four hindlimb muscles (knee flexor, knee extensor, ankle flexor, and extensor) to record the electromyographic (EMG) activity. Body temperature was maintained between 37° and 39° C with a thermostatically controlled heat lamp, 0.9% saline with 8.4 mg/cc sodium bicarbonate and 5% dextrose added was administered IV (~20 cc/hr), and artificial respiration was used to maintain the end tidal CO2 at 3-4%. The carotid arteries were ligated and the left carotid was catheterized to monitor arterial blood pressure. Dexamethasone (2 mg/kg) was administered at the completion of the laminectomy and every 6 hours thereafter for the duration of the experiment. Following surgical preparation, a midcollicular decerebration was conducted and halothane anesthesia

discontinued. At least one hour elapsed between the end of anesthesia and the onset of data collection.

Stimulation

The dura was opened, the levels were identified by root exit, the spinal cord was covered with warm mineral oil, and microstimulation commenced. Vertical, dorsal-to-ventral penetrations were made to position electrodes at locations identified in our previous high-resolution mapping studies to evoke hindlimb motor responses. Activated iridium wire microelectrodes (50 μm diameter) with an exposed electrochemically determined surface area of ~225 μm^2, a 1-3 μm tip, and insulated with Epoxylite were used (IS300, Huntington Medical Research Institutes, Pasadena, CA). Stimuli were charge balanced biphasic pulses with a cathodic phase amplitude of 10-100 μA and duration of 100 μs applied at 40 Hz for 0.5 s. The amplitude of the anodic phase was limited to 100 μA and the duration was set automatically by the stimulator to balance the charge in the primary phase.

Data Collection and Analysis

At selected depths along each penetration the limb was moved on a 3 cm grid of nine to twelve points from a mid-stance position while the stimulation parameters and electrode position were kept constant (see Fig. 4.1). The forces measured at those nine to twelve locations were used to calculate the forces acting on the limb's end-point throughout the workspace [Giszter et al., 1993]. The workspace was divided into triangles, and the forces within a triangle were estimated by a linear interpolation based on the three vectors measured on the vertices (see QPR #2). Note that although we measured forces and moments along three orthogonal axes (x, y and z) our analysis was limited to the sagittal plane. Furthermore, the forces were divided into a passive component (force measured before the onset of activation), and an active component (total forces measured minus the passive portion). Total, active and passive force fields were reconstructed. The forces due to gravity were calculated using simple mechanics and subtracted out. The ankle and knee moments due to gravity were calculated from the cat's weight and segment lengths obtained from post-mortem x-rays [Hoy and Zernicke, 1985]. The torques acting at the knee and ankle joints were calculated from the force measurements by $\mathbf{T}=\mathbf{J}^T\mathbf{F}$, where $\mathbf{T}$ is the torque vector (knee, ankle), $\mathbf{F}$ is the force vector (Fx, Fy), and $\mathbf{J}^T$ is the transpose of the limb's Jacobian. Calculating the Jacobian requires the link lengths (obtained via post-mortem X-rays of the animal), and joint angles (calculated using link length measurements, and the position of the knee joint relative to the force sensor).

The electromyographic (EMG) activity of four hindlimb muscles was measured simultaneously with the evoked forces. EMG was measured from *biceps femoris*, *vastus medialis*, *tibialis anterior*, and *medial gastrocnemius*, and electrode locations were

verified via post-mortem dissection. The raw EMG signals were amplified, filtered (10-1000Hz), and sampled at 2500Hz.

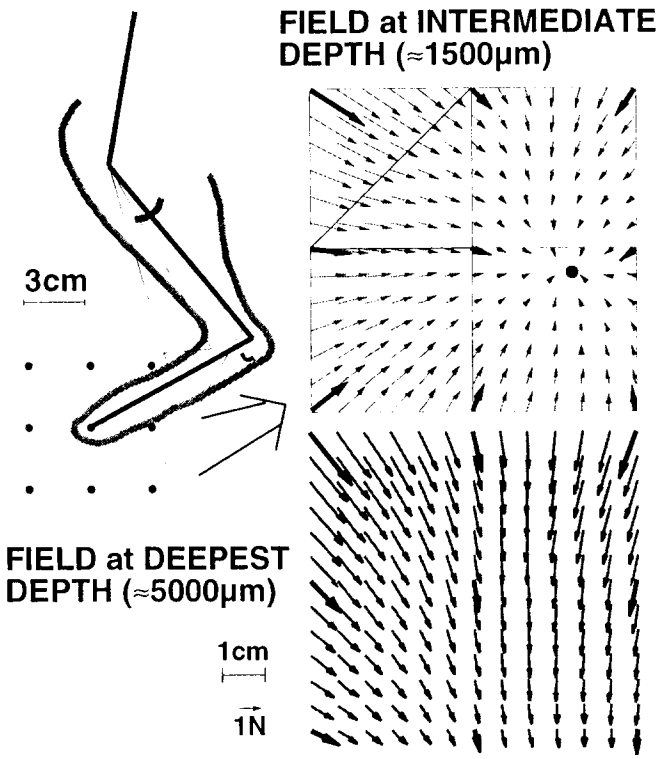

Figure 4.1: Force field construction. Left top: spatial locations where forces were recorded. With the femur held fixed via pins, the knee and ankle were moved through a large range-of-motion (walking range-of-motion shown as thick arc-circles). Right top: actual force vectors measured (thick dark vectors), triangles dividing the workspace, and the interpolated force vectors (thin light vectors). Forces represented are the total forces (active and passive) minus the gravity component. The top right field exhibited convergence, i.e. the net end-point forces go to zero at a location in the workspace, while the bottom field obtained at greater depth did not.

RESULTS

The results reported here were collected over three experiments, all of them using the decerebrate preparation described above. A total of 9 dorsoventral penetrations were performed, and fields were collected at 9 selected depths (one response actually occurred 200 ms after stimulation stopped, and was considered to be a reflex responses; therefore it was not counted as a microstimulation response). The data with contralateral

stimulation from previous experiments were also included in the statistics presented in the figures. This includes an additional 5 contralateral penetrations and 8 fields.

The types of responses found when stimulating contralaterally are shown in Figure 2. Contrary to the results with ipsilateral stimulation, extension responses were more frequent with contralateral stimulation. Caudal and rostral extension responses accounted for 75% of the fields we observed, while the remaining 25% of the responses were flexion withdrawal. Rostal flexion, which occurred once with ipsilateral stimulation, was not observed during contralateral stimulation.

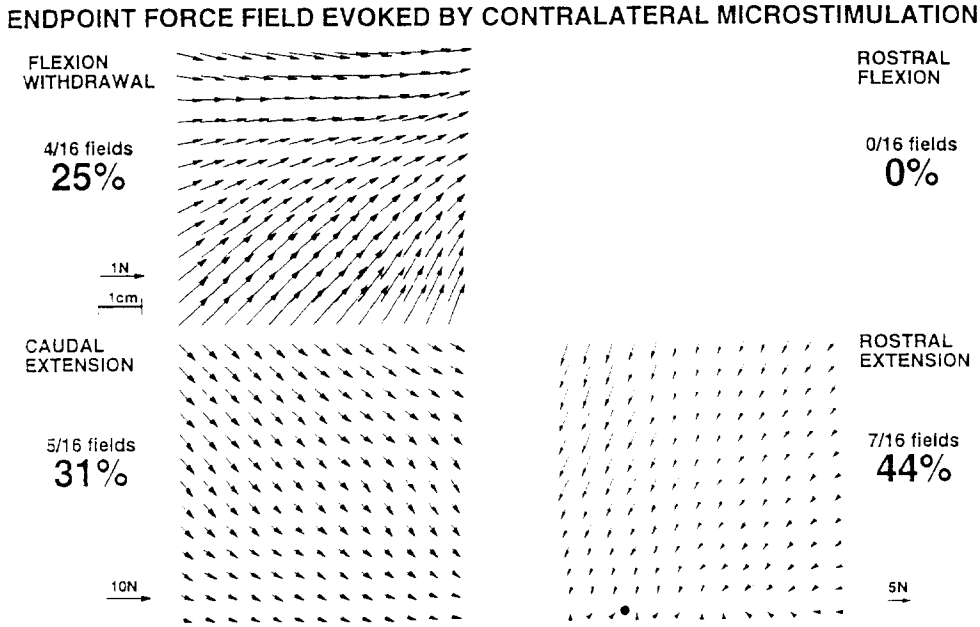

Figure 4.2: Active force fields using stimulation on the side of the cord contralateral to the limb. The relative frequencies at which the fields occurred are also indicated. Top left: Flexion withdrawal, Bottom left: Caudal extension, Bottom right: Rostral extension. Rostral flexion was not observed when stimulation was applied contralateral to the limb (but was observed when stimulation was delivered on the ipsilateral side, see previous quarterly progress report).

A new phenomenon was also discovered: an extensor field with a point of convergence, i.e. a point where the active forces go to zero (see Fig. 4.2 bottom right field). This occurred in one field, but was also observed in the field that developed post-stimulation and was probably a reflex response. The behavior may be part of the natural reflex pattern, and related to the crossed-extension reflex described by Sherrington [Sherrington, 1910], since microstimulation evoked extension in the contralateral limb is

generally accompanied by flexion in the ipsilateral limb (prior to the left hindlimb denervation).

The distribution of the field type with depth is shown in Figure 4.3. Most responses were found at shallow to intermediate depths (800-2000 μm) of penetration, and the majority of responses were in extension. Since we were interested in studying the responses generated by the activation of higher-order neurons, we stopped most penetrations around 4000 μm to avoid motoneuronal regions. Responses may be elicited at greater depths but were not specifically investigated in the experiments reported here.

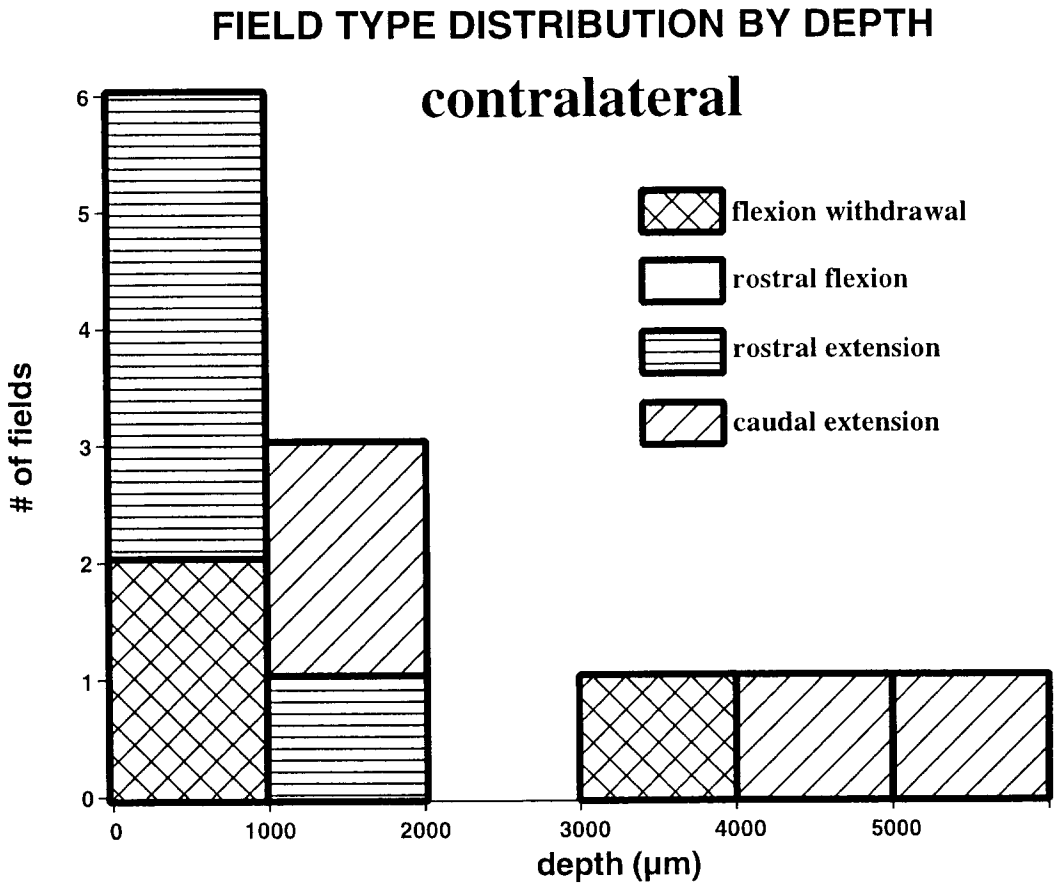

Figure 4.3: Field type distribution by depth for intraspinal microstimulation applied to the side of the cord contralateral to the limb. The height of the bar represents the number of fields found in the depth interval indicated on the horizontal axis.

CONCLUSIONS

Our measurements of endpoint forces in decerebrate, spinal-intact cats indicate that stimulation in the contralateral dorsal and intermediate aspects of the spinal cord generate organized, convergent force patterns, similar to the ones found for stimulation on the ipsilateral side of the cord. The most common response encountered with stimulation in the ipsilateral dorsal aspects of the cord was a flexion withdrawal type of responses, while rostral extension was the most common response for stimulation in the contralateral dorsal aspects of the cord. These results suggest that microstimulation can generate electrically two classical spinal reflexes: flexion withdrawal and crossed extension.

These results also suggest that microstimulation of the mammalian spinal cord can be used to activate groups of muscles to produce organized force patterns at the limb's endpoint. This finding may find application in neural prosthetic control of multi-joint movement in persons with spinal cord injury.

Source Localization for Electrical Mapping of Spinal Neurons

The objective of this project is to develop an intraoperative mapping technique to identify the location of the neurons targeted for stimulation.. We have previously developed techniques for spinal cord mapping in animal models using electrical stimulation as well as immediate early gene expression. However, less invasive methods are required for in vivo mapping.

Therefore, we are undertaking to develop a solution of the inverse problem: given the potentials on the surface of the spinal cord, reconstruct the location of the source that produced those potentials [Oostendorp and Van Oosterom, 1989]. During this quarter we used our previously developed and validate 2-concentric-cylinder volume conductor models of the spinal cord to study the potentials generated on the surface of the spinal cord by intraspinal sources. We also completed a electric field solution for a third model: 2 concentric cylinders with the outer cylinder having anisotropic conductivity, which is more representative of the spinal cord (i.e., accounts for anisotropy of white matter).

METHODS

In the last progress report, we presented the development of two forward models of increasing complexity and increasing similarity to the actual structure of the spinal cord. In our current work we used the second model (fig. 4.4) which consists of two concentric cylinders of differing conductivity, one representing the gray matter the other representing the white matter.

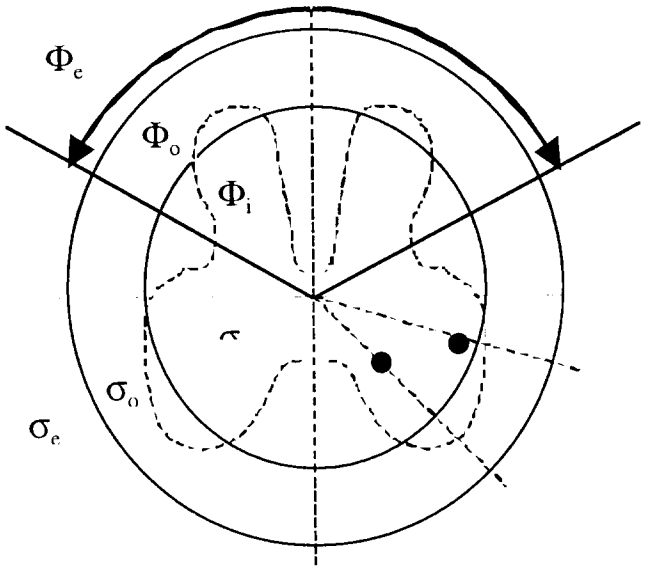

Figure 4.4: The two concentric cylinders volume conductor model of the spinal cord. Illustrated above is the approximate feasible surface recording region of the spinal cord. The second forward model is used (inner radius of 2cm and outer radius of 3cm). An outline of the gray matter is also shown to illustrate the model approximation of reality. The two points in the figure are used in the model as locations of motor nuclei and results are shown for source in these locations in figures 4.5 and 4.6.

The analytical solution for this model was implemented in MATLAB using a Fourier solution method (see QPRs 2 and 3 for details). This solution was used to calculated the surface potentials that were generated by point current sources at two different locations within the gray matter.

RESULTS

The surface potentials calculated using the second forward model, for two different source locations, are shown in figs. 4.5 and 4.6. The two source locations are shown in fig. 4.4 as black dots at $\theta = 45^0$ and $\theta = 78.75^0$. Note that the potential has a strong maximum at the surface directly overlying the source location. However, this is outside the region where it will be feasible to make experimental recordings of the surface potential. Within the feasible region, there is a large potential gradient in the z-direction (longitudinal, parallel to spinal cord), but very little change in potential in the

theta (circumferential direction). The potential gradient with changes in theta only occurs for z coordinate at the source.

CONCLUSION

These results demonstrate that the potentials recorded on the surface of the spinal cord will be of a sufficient magnitude to make surface recording of evoked potentials feasible (~10mV/μA of source current). The spatial distribution of potentials suggest that the recording array should have multiple electrodes in z, to capture the large potential gradient in z, but that there is little potential gradient in theta.

Surface potential Contour Map for Source at $\theta = 45^0$, ρ = 1cm

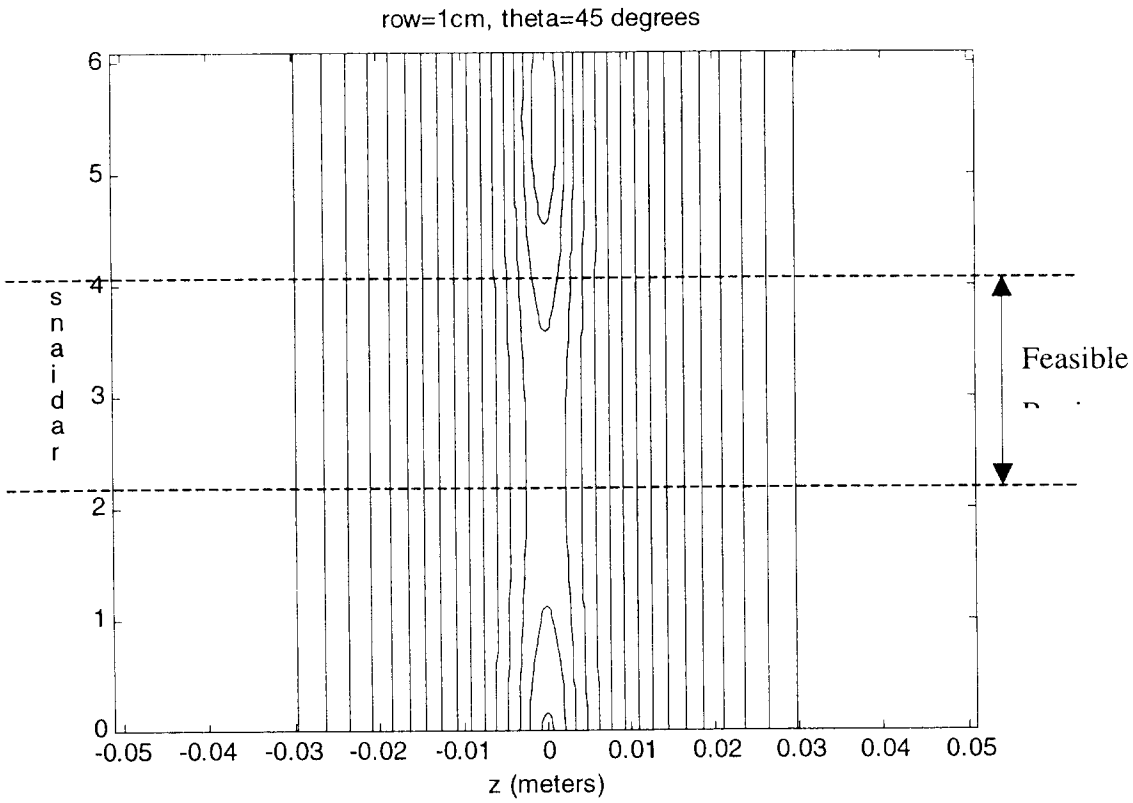

Figure 4.5: Contour map of spinal cord surface potentials for a 1mA source at $\theta = 45^0$, ρ = 1cm. The model assumes a *very low* conductivity outside the cord (mineral oil conductivity of $2x10^5$ S/m) accounting for seemingly high voltage levels. The contours span potentials from 10 to 95 Volts in increments of 5 Volts/contour. The feasible recording region is illustrated; it suggests that recording at the edges of the feasible region will probably be very important.

Surface potential Contour Map for Source at $\theta = 78.75^0$, ρ = 1cm

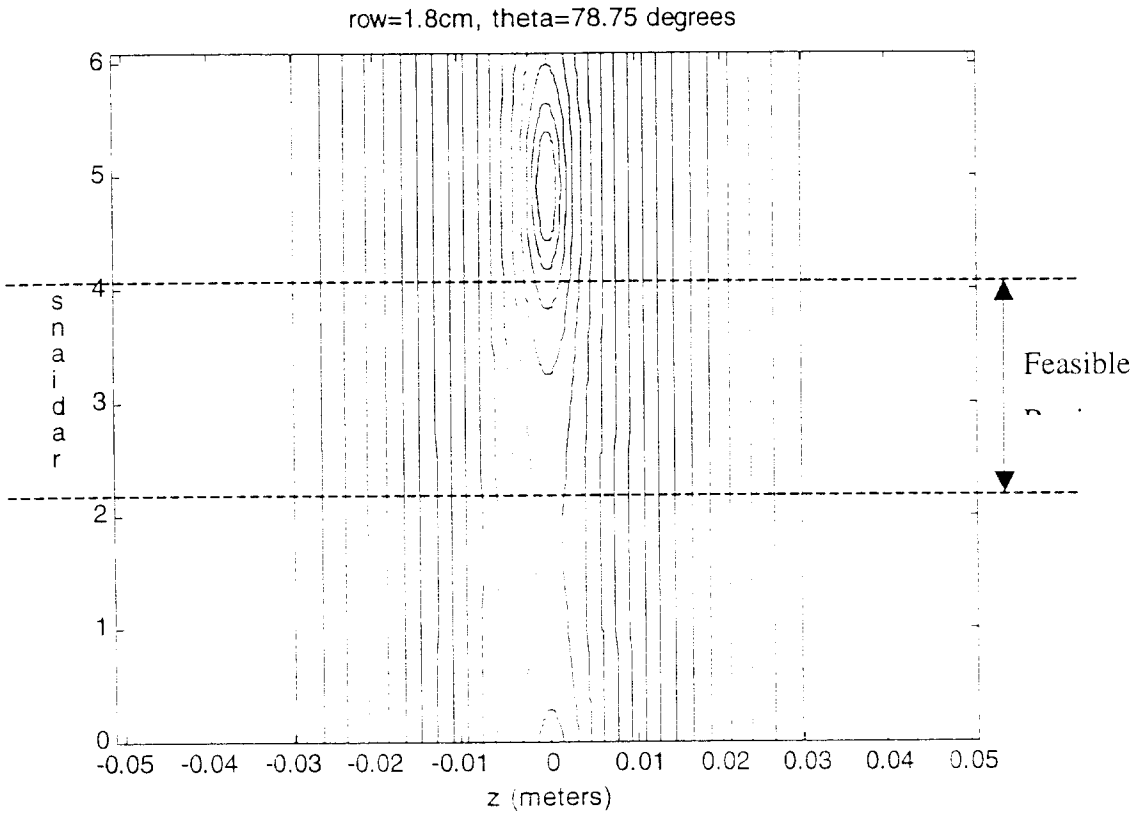

Figure 4.6: Contour map of spinal cord surface potential for a 1mA source at $\theta = 78.75^0$, ρ = 1.8cm. This simulation was run with the same conductivity parameters as in fig. 4.5; the contours represent the same range and levels as well. This stimulus is closer to the recordable region of the surface, which make a significant difference. Both this figure and the previous suggest that recording at the appropriate z-level is also *very* important.

PUBLICATIONS THIS QUARTER

Grill, W.M., N. Bhadra, B. Wang (1999) Bladder and urethral pressures evoked by microstimulation of the sacral spinal cord in cats. Brain Research 836:19-30.

OBJECTIVES FOR THE NEXT QUARTER

In the next quarter we will continue our co-localization studies to identify inhibitory spinal neurons active during micturition. Although not discussed in this report, we have been working to identify suitable antibodies and dilutions for immunocytochemical detection of c-Fos [Grill et al., 1998] with glycine, the primary inhibitory neurotransmitter in the spinal cord. We will continue this work in the next quarter.

We will also continue our studies characterizing the hindlimb motor responses to lumbar microstimulation. Our specific objective is to complete the assembly of a two degree-of-freedom robot that will enable measurement of forces and positions during hindlimb motion. The device will allow us to investigate the effects of limb movement on the forces produced by microstimulation, and to measure the limb's response to controlled perturbations. The device will thus allow us to characterize the dynamic nature of the intraspinal response, which will complete the static characterization accomplished to date.

Finally, we will continue development of our electrical mapping method. Our specific objective is to implement and verify the solution for of the third forward model.

LITERATURE CITED

Giszter, S.F., F.A. Mussa-Ivaldi, E. Bizzi (1993) Convergent force fields organized in the frog's spinal cord. J. Neuroscience 13:467-491.

Grill, W.M., B. Wang, S. Hadziefendic, M.A. Haxhiu (1998a) Identification of the spinal neural network involved in coordination of micturition in the male cat. Brain Research 796:150-160.

Hoy, MG and RF Zernicke. "Modulation of limb dynamics in the swing phase of locomotion." J Biomech. 18(1 1985): 49-60.

Oostendorp, T.F., A. Van Oosterom (1989) Source parameter estimation in inhomogeneous volume conductors of arbitrary shape. IEEE Trans. Biomed. Eng. 36:382-391.

Sherrington, CS. "Flexion-reflex of the limb, crossed extension reflex and reflex stepping and standing." Journal of Physiology. 40(1910): 28-121.